IEEE Access
Multidisciplinary | Rapid Review | Open Access Journal

Received August 19, 2019, accepted September 9, 2019, date of publication September 13, 2019,
date of current version December 13, 2019.

Digital Object Identifier 10.1109/ACCESS.2019.2941240

Two-Layer Collaborative Architecture for Distributed Volt/Var Optimization and Control in Power Distribution Systems

QIYI YU[1], QI WANG[1], (Member, IEEE), WEI LI[2], (Member, IEEE), FUSUO LIU[2], (Member, IEEE), ZHONGYU SHEN[1], (Member, IEEE), AND JIAQI JU[1]

[1]School of NARI Electric and Automation, Nanjing Normal University, Nanjing 210046, China
[2]NARI Group Corporation, Nanjing 210046, China

Corresponding author: Qi Wang (wangqi@njnu.edu.cn)

This work was supported by the 2018 Postgraduate Research and Innovation Project of Jiangsu under Grant KYCX18_1229.

ABSTRACT For large-scale distribution networks (DNs) with distributed generations (DGs), the conventional centralized Volt/Var optimization and control (VOC) have high demand for online computing resources and efficiency. This paper proposes a new decision-making method for the distributed VOC (D-VOC) based on a two-layer collaborative architecture. First, for a distributed equivalent load system with on-load tap changer (OLTC), this paper studies how to minimize the active power loss and reach the target voltage of load side for the equivalent load system. Second, a concept of virtual soft controller (VSC) is presented based on the distributed equivalent load system, and the local optimal control strategies of VSCs are designed to realize the D-VOC in DNs. On this basis, a two-layer collaborative architecture for the D-VOC is designed. VSCs could be built in virtual or real deployment at nodes where reactive power sources or reactive power compensation devices are equipped, and they are at the bottom layer of the architecture. VSCs upload their distributed decision results to the local control center (LCC) which is at the top layer of the architecture. The LCC systematically verifies and authorizes each VSC to execute its own operational instruction. Case study on the modified PG & E 69-bus distribution grid shows that the method is feasible and has satisfactory efficiency.

INDEX TERMS Distribution network, distributed optimization and control, reactive power, voltage, two-layer architecture, virtual soft controller.

I. INTRODUCTION

The rapid growth of the national economy and the improvement of people's living standards have led to the increase of electricity demand, resulting in series of problems such as system stability, power quality and reactive power optimization [1]. The fossil energy is exhausting and the environment problem is more serious. Renewable energy generation (REG) has become an international research hotspot because it is clean, environmentally friendly, and low-cost. Compared with thermal or hydro power generation, however, REG is intermittent and uncertain, and poses well-known technical challenges for power network operation [2]–[4].

The associate editor coordinating the review of this manuscript and approving it for publication was Feng Liu.

The conventional distribution network (DN) is a radial system with unidirectional power flow. Because of the high proportion of distributed generation (DG), the characteristic of reactive power and operation condition have changed dramatically in DN [5]. In particular, voltage deviation and overload will seriously affect the stability and reliability of network [6]–[8]. It is difficult and expensive to tackle these problems through upgrading lines and increasing Var equipment. Therefore, it is necessary to study new method of Volt/Var optimization and control (VOC) to solve series of problems for high proportion integration of DGs [9], [10].

It is obvious that approaches to VOC can mainly be classified into two categories: centralized and distributed strategies.

The most widely used approach is centralized strategy. For centralized strategy, some approaches are mostly based on traditional algorithms such as linear programming [11],

nonlinear programming [12] and interior-point method [13]. Others are based on the artificial intelligent algorithms, such as genetic algorithm [14], simulated annealing algorithm [15], and particle swarm algorithm [16]. In common, optimization problem with centralized strategy is solved by distribution management system (DMS) [17] in a control center. The control center acquires measurement data of nodes, the settings of on-load tap changer (OLTC), the set number of capacitor banks, the reactive power output of static var compensator (SVC) and so on. The optimization algorithm is used to solve optimal reactive power flow problems, and the optimal decision results are sent to Var equipment through remote terminal units [18]. It turns out that the centralized strategies aim at system global optimization. For small-scale DNs with unidirectional power flow, it is theoretically possible to obtain the accurate optimal solutions. However, there are various drawbacks that might impede the use of centralized strategies in future [19]. First, the increase of uncertainties (due to distributed REGs, electric vehicles, and distributed energy storage system (DESS)) will make the use of the centralized strategy difficult. The amount of data that needs to be measured and collected increases the burden on the communication system and the difficulty of security defense. Second, the control center acquires a large amount of data which relies on a perfect communication network and consumes more storage space. The high demand for online computing resources and efficiency must be met when the algorithm is used for centralized strategy. If the delay due to the data acquisition and transmission is taken into account, the actual operating efficiency may be lower. Third, all measurement data needs to be transmitted to the central control system. Once the central control system is out of order, the entire management system will collapse. Consequently, for centralized strategies, it is difficult to fully comply with the trends of DNs [20].

Decentralized control [21] is a distributed decision-making strategy by controlling Var equipment (such as OLTC, shunt capacitor bank, SVC, static var generator (SVG), and DG); at the same time, through the interaction of a small amount of key information between the various parts of the network, the decentralized structures can accomplish the distributed VOC (D-VOC).

Based on sensitivity analysis, an architecture for the distributed Volt/Var control is proposed that relies on controlling reactive power injections provided by DG [22]–[24]. In [25], a real-time voltage control scheme is proposed by using DGs which combines a local and a centralized control of their reactive powers. The local control provides fast response after a disturbance enhancing voltage quality, and the centralized control uses measurements collected throughout the network to keep voltages within specified limits and balance the various DG contributions. Based on the model predictive control, [26] proposed a centralized control scheme that was solved in a distributed fashion through the Lagrangian decomposition algorithm. In addition, the multi-agent system (MAS) is one of the important methods of distributed control [27]–[29]. In [27], the optimization objectives include maintaining the system voltage within a specified range, minimizing system loss, and reducing the switching of shunt capacitors. To achieve these objectives, the shunt capacitor agent and voltage regulator agent work collaboratively by using forward/backward sweep method. In [28], a hierarchical approach is proposed based on distributed multi-agent systems. The approach combines the primary voltage control provided by the decentralized controllers of DGs and OLTCs with a secondary voltage control layer that implements a gossip algorithm in a MAS approach. In [29], the DN is divided into multi-regions, and the DESS is used as the control agent. The proposed partitioning algorithm decomposes the DN into multi zones, and each one is under the control of a single DESS.

In summary, the distributed decision-making strategy eases the pressure in computation of the centralized strategy in DMS for the VOC. Nevertheless, due to the intermittence and uncertainty of DGs and loads, DMS faces difficulties in some applications when global information may not be available or accurate [30]. Under this condition, if a local controller is allowed to perform actions independently, it may affect the operation of other controllers, Var equipment, or even the entire system. Accordingly, it is also necessary to design an appropriate coordination strategy to standardize the operation of each controller.

This paper proposes a new decision-making method for the VOC in a two-layer collaborative architecture. The virtual soft controllers (VSCs) at the bottom layer can autonomously make distributed decisions which must be verified and be authorized to execute their operational instructions by an algorithm module of DMS in the local control center (LCC) at the top layer. In the new collaborative architecture, the ''top layer'' is responsible to supervise VSCs and inspect whether the effect of distributed decision-making is positive, whether system constraints are violated by VSCs, whether VSCs can be allowed to execute their operational instructions respectively and so on.

The distributed optimization results of VSCs are obtained by the distributed optimization algorithm proposed in this paper. Compared with the centralized optimization, the distributed optimization algorithm proposed in this paper occupies fewer computing resources and has a satisfactory performance of fast computation speed. Moreover, in the optimization process, several VSCs at the bottom layer can accomplish optimization calculations in a parallel and independent manner, and thus further improve the computing speed. Therefore, the proposed method can generate distributed control strategies in a short time, thereby achieving the aim of improving the voltage profile and reducing system loss.

The major contributions of this paper are listed as follows:

1) A new two-layer collaborative architecture for the D-VOC is designed. VSCs are deployed in virtual or real mode at the bottom layer, which are primarily responsible for local decision-making calculating and/or decision execution.

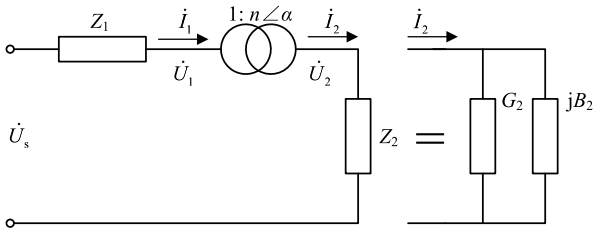

FIGURE 1. Equivalent load system with OLTC.

The top layer is deployed in LCC which is primarily responsible to verify and authorize decision results uploaded by VSCs.

2) A distributed decision-making algorithm for VSC is proposed. The algorithm can minimize the active power loss and reach the target voltage at load node for a distributed equivalent load system with OLTC.

3) Based on the two-layer collaborative architecture and the distributed decision-making algorithm, the process of interaction between the top layer and the bottom layer is designed, and a new scheme for the multi-period decision-making is proposed. The scheme can accomplish the rough and fine optimization in two stages respectively for the long and short periods, which can not only simplify calculation but also obtain the results of loss reduction and voltage control.

The remainder of this paper is organized as follows. Section II gives an equivalent load system with OLTC, and Section III analyzes target voltage at load side and the minimization of active power loss of the equivalent system. Section IV describes a concept of VSC, a local distributed controller. The control scheme of VSC which involves decision-making strategies and optimization algorithm is designed for the D-VOC. Section V designs a two-layer collaborative architecture for the VOC. Moreover, according to the idea of distributed control, the virtual or actual deployment scheme of VSC is designed and the access to execute its own operational instruction is set. Section VI describes a case study on the modified PG & E 69-bus distribution grid.

II. EQUIVALENT LOAD SYSTEM WITH OLTC

In a radial DN, the equivalent load power at a node is the sum of the local load power of the node and the equivalent load power of its downstream subsystem. The equivalent impedance and admittance of the equivalent load is $Z_2 = R_2 + \mathrm{j}X_2$, and $Y_2 = G_2 + \mathrm{j}B_2 = 1/Z_2$ respectively.

Without loss of generality, assume that the equivalent load is connected to the secondary terminal of an ideal transformer and the primary terminal is connected to the upstream equivalent source. The equivalent circuit is shown in Fig. 1.

In Fig. 1, voltage and current phasor at the secondary terminal of OLTC is $\dot{U}_2$ and $\dot{I}_2$ respectively; voltage and current phasor at the primary terminal is $\dot{U}_1$ and $\dot{I}_1$ respectively; transformation ratio is $1:n\angle\alpha$, where n is related to tap position of OLTC, and α, a constant, is related to connection mode; voltage phasor of equivalent source is $\dot{U}_s$; the branch impedance is $Z_1 = R_1 + \mathrm{j}X_1$, including the impedance of feeder line and the primary winding of OLTC.

III. FUNDAMENTAL FORMULAS OF EQUIVALENT LOAD SYSTEM

For an ideal transformer, voltage and current phasor satisfy the following conditions:

$$\dot{U}_2 = n\mathrm{e}^{\mathrm{j}\alpha}\dot{U}_1 \tag{1}$$

$$\dot{I}_2 = (1/n)\,\mathrm{e}^{\mathrm{j}\alpha}\dot{I}_1 \tag{2}$$

$$\begin{cases} \dot{U}_2 = \dot{I}_2 Z_2 \\ \dot{U}_1 = \dot{I}_1\left(Z_2/n^2\right) \end{cases} \tag{3}$$

Output current and apparent power of the equivalent source can be calculated:

$$\dot{I}_1 = \dot{U}_s/\left(Z_1 + Z_2/n^2\right) \tag{4}$$

$$S = \dot{U}_s\hat{I}_1 = U_s^2/\left(\hat{Z}_1 + \hat{Z}_2/n^2\right) \tag{5}$$

With $K = 1/n^2$, splitting real and imaginary parts of (5) yields (6).

$$\begin{cases} P = \left[R/(R^2+X^2)\right]U_s^2 \\ Q = \left[X/(R^2+X^2)\right]U_s^2 \end{cases} \tag{6}$$

where $R = R_1 + KR_2$, and $X = X_1 + KX_2$.

A. MINIMIZATION OF ACTIVE POWER LOSS FOR THE EQUIVALENT LOAD SYSTEM

For the equivalent load system, the minimization of active power loss is equivalent to the minimization of P in (6). Therefore, the following analysis only focuses on minimum P.

From the first sub-formula of (6), we observe that the physical variables affecting P by means of compensation or regulation are: 1) U_s, the voltage of the equivalent source; 2) K, related to the ratio n of OLTC; 3) the Var compensation of capacitor bank, SVG and SVC (mainly related to B_2).

When other physical variables are fixed, P decreases monotonously with the decrease of U_s. However, U_s can be slightly decreased within voltage limit on the condition that load distribution and voltage control are not impacted. Therefore, in the following, the adjustment of U_s is mainly used as an auxiliary means of load voltage control when local Var compensation and OLTC are limited. As for loss reduction, controlling the voltage U_s should be used moderately when capability of voltage control is sufficient.

Based on the above analysis, the following will focus on the other two factors to minimize P.

1) K-VALUE CONDITION FOR MINIMUM P

Based on the first sub-formula of (6) and the necessary condition $\partial P/\partial K = 0$ for minimum P, (7) can be deduced.

$$(R/X)^2 + 2\,(X_2/R_2)\,(R/X) - 1 = 0 \tag{7}$$

Furthermore,

$$R/X = -X_2/R_2 \pm \sqrt{(X_2/R_2)^2 + 1} \triangleq C \tag{8}$$

In (8), if $R_2 > 0$ and $X_2 > 0$, then the sign "±" is plus sign "+"; if $R_2 > 0$ and $X_2 < 0$, the sign "±" is minus sign "−". In the actual calculation, K is determined by (9) and the positive value closest to 1.0 can be selected as the final result of K.

$$K = -(R_1 - CX_1)/(R_2 - CX_2) \tag{9}$$

2) B_2-VALUE CONDITION FOR MINIMUM P

In addition to changing K, controlling Var equipment (i.e., changing B_2) at the load side can minimize P.

Based on the first sub-formula of (6), the B_2-value condition for minimum P is:

$$\frac{\partial P}{\partial B_2} = \frac{\partial P}{\partial R_2}\frac{\partial R_2}{\partial B_2} + \frac{\partial P}{\partial X_2}\frac{\partial X_2}{\partial B_2} = 0 \tag{10}$$

From (6) and (10), (11) can be deduced.

$$B_2 = (R/X)\, G_2 \text{or } B_2 = -(X/R)\, G_2 \tag{11}$$

Because the right of the equal sign in (11) is a non-linear implicit function, it is difficult to be solved directly. $B_{2\text{new}}$ can be determined by the iterative formula (12), where the variable q is the iteration number for computing B_2. The derivation process of (12) is described in Appendix C, and the reason for minimizing P by (9) and (12) in Appendix D.

$$B_{2,(q)} = \begin{cases} \dfrac{R_1(G_2^2 + B_{2,(q-1)}^2) + KG_2}{X_1(G_2^2 + B_{2,(q-1)}^2) - KB_{2,(q-1)}} G_2 \\ -\dfrac{X_1(G_2^2 + B_{2,(q-1)}^2) - KB_{2,(q-1)}}{R_1(G_2^2 + B_{2,(q-1)}^2) + KG_2} G_2 \end{cases} \tag{12}$$

If $|B_{2,(q)} - B_{2,(q-1)}| \le \varepsilon_B$ (ε_B is convergence threshold.), the convergence result $B_{2\text{nw}}$ is obtained by (12).

The final B_2-value of (12) is determined according to the following rules:

a) If $R_2 > 0$ and $X_2 > 0$, then $B_{2\text{nw}} > B_{2,(q=0)}$;
b) If $R_2 > 0$ and $X_2 < 0$, then $0 < B_{2\text{nw}} < B_{2,(q=0)}$;
c) If $R_2 < 0$ and $X_2 > 0$, then $B_{2\text{nw}} > B_{2,(q=0)}$.

3) K-VALUE AND B_2-VALUE JOINT CONDITIONS FOR MINIMUM P

We use (9) and (12) to calculate K and B_2 iteratively. The convergence condition is the same as the condition in Section IIIA 2). The convergence solution corresponds to the joint conditions for minimum P.

B. TARGET VOLTAGE CONTROL FOR THE EQUIVALENT LOAD SYSTEM

We obtain (13) by substituting $K = 1/n^2$ into (4):

$$\dot{I}_1 = \dot{U}_s/(Z_1 + KZ_2) \tag{13}$$

Then, substitute (13) into (2).

$$\dot{I}_2 = \sqrt{K}e^{j\alpha}\dot{I}_1 = \sqrt{K}\dot{U}_s e^{j\alpha}/(Z_1 + KZ_2) \tag{14}$$

The voltage at the secondary terminal of OLTC is:

$$\dot{U}_2 = \dot{I}_2 Z_2 = \sqrt{K}\dot{U}_s e^{j\alpha} Z_2/(Z_1 + KZ_2) \tag{15}$$

Its amplitude is:

$$U_2 = \sqrt{K}U_s/|K + Z_1/Z_2| \tag{16}$$

(16) shows that:

1) U_2, the voltage of load node, is mainly related to K, U_s, Z_2 and so on.

2) Controlling Var equipment at the load side (including shunt capacitor banks, SVC, SVG, and other dispersed Var equipment), namely changing the B_2-value, is a means of local voltage control;

3) Changing the tap position of OLTC is a means of local voltage control;

4) Controlling Var equipment at the power supply side (including shunt capacitor banks, reactors, SVC, SVG, and dispersed Var equipment which have an effect on U_s), namely changing the value of U_s is a means of remote control of U_2.

IV. LOCAL DECISION-MAKING SCHEME BASED ON THE EQUIVALENT LOAD SYSTEM

A. D-VOC STRATEGIES

Section III has analyzed the minimization of active power loss and the target voltage control for the equivalent load system with OLTC. Considering both loss minimization and voltage control, this section will continue to analyze the local decision-making scheme for the D-VOC in DNs.

For the equivalent load system with Var equipment in Fig. 1, assume that a VSC is deployed corresponding to the equivalent load system with Var equipment and is assigned with different functions such as "local measurement, local decision-making, and local execution", "local measurement, local decision-making, remote check, and remote regulation" or "local measurement, local decision-making, remote check, and local execution". VSCs with this ability of distributed decision-making can be incorporated into the two-layer collaborative architecture for the D-VOC in Section V. The following will first describe the decision-making process of VSC.

According to Section III, the relationship of voltage control at load side is coincided with (16), in which U_s, K, and B_2 are the key parameters not only affecting U_2, but also affecting the minimization of P. When VSC makes decisions locally, it is necessary to coordinate the compensation or control measures related to U_s, K, and B_2 to meet the demand for VOC.

For the object voltage at load node $U_{2\text{obj}} \in [U_{2\min}, U_{2\max}]$, the relationship among U_s, K and B_2 is:

$$U_2 = \sqrt{K}U_s/|K + Z_1/Z_2| = U_{2\text{obj}} \tag{17}$$

Based on the local balance principle of reactive power, in view of operation cost and convenience, the VSC's local decision-making scheme is designed. The scheme is split into two parts for different control objectives as follows:

1) U_2 must be strictly kept at the target voltage $U_{2\text{obj}}$.

Assume that LCC gives a strict instruction of target voltage control at load side (which can be issued by dispatcher or calculated by traditional centralized optimization module), and then the decision-making process of VSC is listed as following:

[a] Local Var compensation is used preferentially to make U_2 close to $U_{2\text{obj}}$ by changing B_2.

Based on $B_{2\text{new}}$ calculated by (17) in the case of other variables fixed, control increment for Var equipment or control mode can be determined as follow:

For the shunt capacitor banks, set number of switched capacitors is selected according to $\Delta B_2 = B_{2\text{new}} - B_{2\text{old}}$. For SVC or SVG in constant-reactive-power mode (Q_{const} mode), control increment of Q_2 is obtained according to $\Delta Q_2 = B_{2\text{new}}U_{2\text{obj}}^2 - B_{2\text{old}}U_{2\text{old}}^2$ (where $U_{2\text{old}}$ is the voltage after the last iteration) with considering the reactive power limit. For SVC or SVG in constant-voltage mode (V_{const} mode), if ΔQ_2 is within the limit $\Delta Q_{2\max}$ (which is the maximum variation of the output of SVC/SVG), the target value of U_2 can be directly set to $U_{2\text{obj}}$; if ΔQ_2 exceeds the limit, the control mode is converted into the constant-reactive-power mode, and target value of ΔQ_2 is set to its limit $\Delta Q_{2\max}$. Meanwhile, the information that control mode is converted and output is out of reactive power's limit is uploaded to LCC.

[b] If the deviation between $U_{2\text{obj}}$ and $U_{2\text{new}}$ (which is the voltage after local Var compensation and calculated by power flow calculation in LCC) still exceeds the set threshold $U_{2\varepsilon}$, then the tap setting of OLTC will be adjusted.

In this case, $B_{2\text{new}}$ is substituted into (17) to calculate the K_{new} of K with other variables constant. According to the K_{new}, the tap setting of OLTC is selected.

[c] If the deviation between $U_{2\text{obj}}$ and $U_{2\text{new}}$ after local compensation and tap adjustment still exceeds $U_{2\varepsilon}$, the increment of U_s can be calculated by (17). Through the two-layer collaborative architecture in Section V, the corresponding VSC uploads this information to LCC. And it requests LCC to issue the operation instructions that adjust the relevant Var equipment at upstream or downstream of corresponding VSC to make U_s equal to the target value.

Fig. 2 mainly shows the decision-making process of different types of VSCs, which includes: some VSCs have the functions of self-checking and self-decision; others only have the function of distributed computing, and the results of VSCs need to be verified by LCC. The process of check in LCC is: after VSC sends result to LCC, LCC checks whether the voltage reach the target value based on power flow calculation. The specific functions of VSC are determined by LCC, which will be described in Section V.

2) U_2 is not strictly kept at the target voltage $U_{2\text{obj}}$.

In this case, VSC is allowed to minimize the active power loss for the equivalent load system with $U_2 \in [U_{2\min}, U_{2\max}]$, or the corresponding VSC accepts other nearby VSC's request information from LCC. The decision-making process of VSC is as following (shown in Fig. 3):

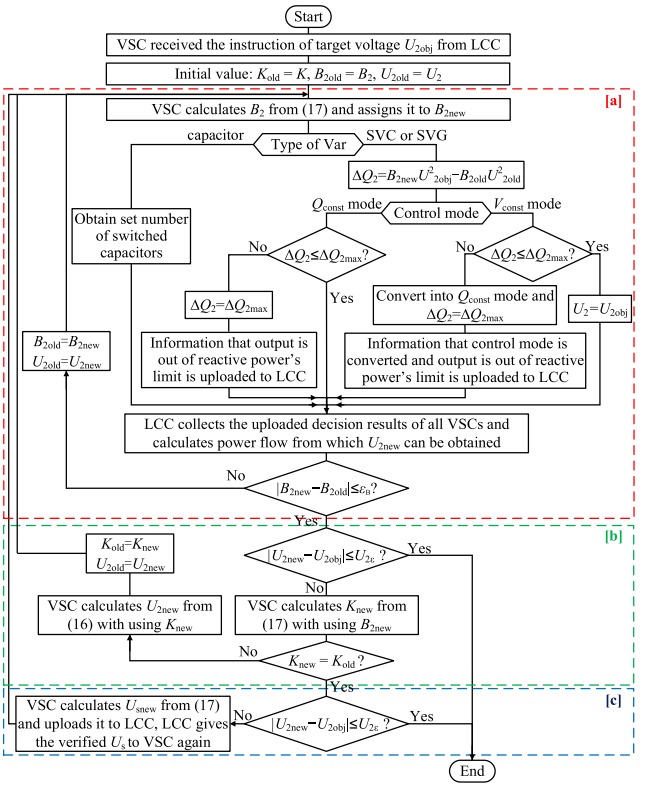

FIGURE 2. The VSC's decision-making process of voltage target control.

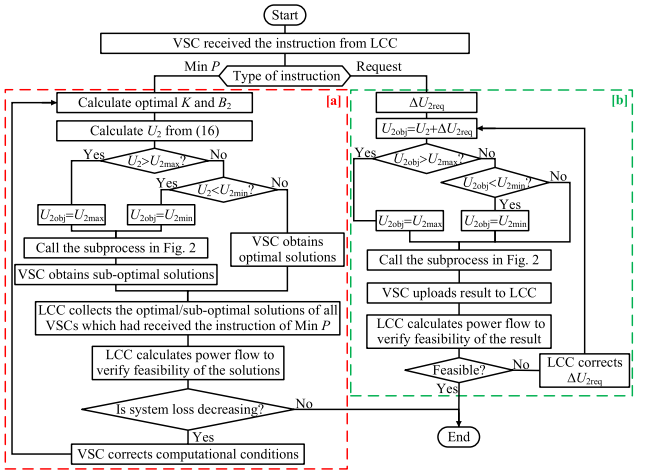

FIGURE 3. The VSC's decision-making process of minimizing the active power loss.

[a] If $U_2 \in [U_{2\min}, U_{2\max}]$ and Var equipment has enough capacity margin, then VSC can perform process of minimization of active power loss.

For different types of Var equipment involving in the distributed optimization, VSC calculates the optimal solutions of K and B_2 for minimum P according to Section III, and LCC verifies their feasibility:

Substitute the optimal solutions of K and B_2 into (16) to calculate U_2. If $U_2 \in [U_{2\min}, U_{2\max}]$, then the optimal solution is feasible. If U_2 exceeds constraint, then it is set

to the limit and is substituted into (16) to calculate the sub-optimal solutions of K and B_2.

LCC checks whether active power loss of system is minimum and voltage exceeds limit by power flow program. If $U_2 \in [U_{2\min}, U_{2\max}]$ and P decreases in the iterative process, VSCs continue to change the increment of variable in the distributed computation. If $U_2 \in [U_{2\min}, U_{2\max}]$ and P increases in the iterative process, the distributed computation ends temporarily.

[b] LCC sends other nearby VSC's request information to this VSC.

In this case, the requester may be the downstream node or the upstream node of VSC. Regardless of upstream or downstream, this VSC only needs to calculate the corrected B_2 or K and its relevant control increment through (17) based on the request information (including adjustment $\Delta U_{2\text{req}}$), voltage limit, and reactive power margin of Var equipment (The related content is described in 1) of Section IV-A.).

Generally, the priority of [b] is higher than [a] of 2) in Section IV-A, so this VSC should preferentially respond to the request from other VSCs (same as the process in [b]). If there is no request for voltage regulation, then this VSC makes decision [a] of 2) to minimize loss.

B. MULTI-PERIOD DECISION-MAKING SCHEME

Var equipment (such as DG, SVG and SVC) controlled by power electronic devices can quickly respond to the control instructions. Moreover, the single-time cost of control is negligible, for their controllable times is enough in total. Consequently, when DG, SVG and SVC participate in multi-period optimal decision-making, influence of time couple and control cost can be neglected. However, OLTC and shunt capacitor bank with mechanical switch have some shortcomings such as slow response to control instructions, long execution time and wear life-span. Therefore, the daily action times and the interval between two actions should be constrained.

The variability of load (including DG) is the main factor affecting the regulation of OLTC and shunt capacitor banks. If the operation ways are reduced moderately, (for instance, 96 or 48 short time periods are merged into a few long time periods which may be unequal periods), then the daily action times will shorten and the interval between two actions will grow longer.

Generally, extend from a selected initial short period (in Fig. 4) to the left or right along the net load (which equals load minus DG) curve. If the absolute value of power deviations of short periods relative to start short period is less than or equal to the setting power span P_{span}, all the short periods will be merged into a long period. The ending of this long period will become a new starting point of the next long period to be merged. This process lasts until the daily load cure is fully merged. The operation ways of the long period after mergence can be reduced into one way, and its average

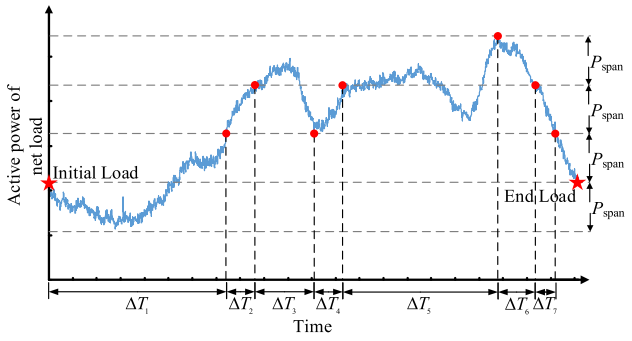

FIGURE 4. Reduction of operation ways and mergence of periods.

power is:

$$\bar{P}_k = \frac{1}{\Delta T_k}\sum_{i=1}^{N_k}(P_i\Delta t) = \frac{1}{N_k\Delta t}\sum_{i=1}^{N_k}(P_i\Delta t) = \frac{1}{N_k}\sum_{i=1}^{N_k}P_i \tag{18}$$

where N_k is the number of short periods in the k^{th} long period; Δt is the length of the short period; ΔT_k is the length of the k^{th} long period, namely $\Delta T_k = N_k\Delta t$; P_i is the load power of the i^{th} short period in the k^{th} long period.

If the number of long periods after merging is M, then

$$N = \sum_{k=1}^{M} N_k \tag{19}$$

where N is the number of short periods, and usually equal to 96, 48 or 24 that correspond to $\Delta t = 15$, 30 or 60.

Thus, the original series $\{P_i | \, i = 1, 2, \ldots, N\}$ with equal interval (Δt) are transformed into a new series $\left\{\bar{P}_k \middle| \, k = 1, 2, \ldots, M\right\}$ with unequal intervals.

The characteristics of the above method are:

1) For the same load curve, the larger P_{span} is, the higher the degree of operation way reduction is.

2) For the same P_{span}, the larger the load rate (i.e., the ratio of average load power to peak load) is, the higher the degree of operation way reduction is.

Consequently, the load curve can be merged by changing P_{span} in consideration of the interval constraint between two actions for the capacitor and OLTC.

Γ_{oltc} and Γ_{cap} are the minimum interval between two actions respectively for OLTC and capacitor. The length of long period should satisfy the constraint

$$\min_{k=1\sim M} \Delta T_k \geq \max\{\Gamma_{\text{oltc}}, \Gamma_{\text{cap}}\} \tag{20}$$

If the period merging result dissatisfies (20), P_{span} appropriately increases to correct the merging result until (20) is satisfied. Reduction of operation ways could only be determined after the merging result is verified by (20).

Generally, Γ_{oltc} is larger than Γ_{cap}. Considering that (20) may cause ΔT_k too long and the optimization less elaborate, (20) can be relaxed to

$$\min_{k=1\sim M} \Delta T_k \geq \Gamma_{\text{cap}} \tag{21}$$

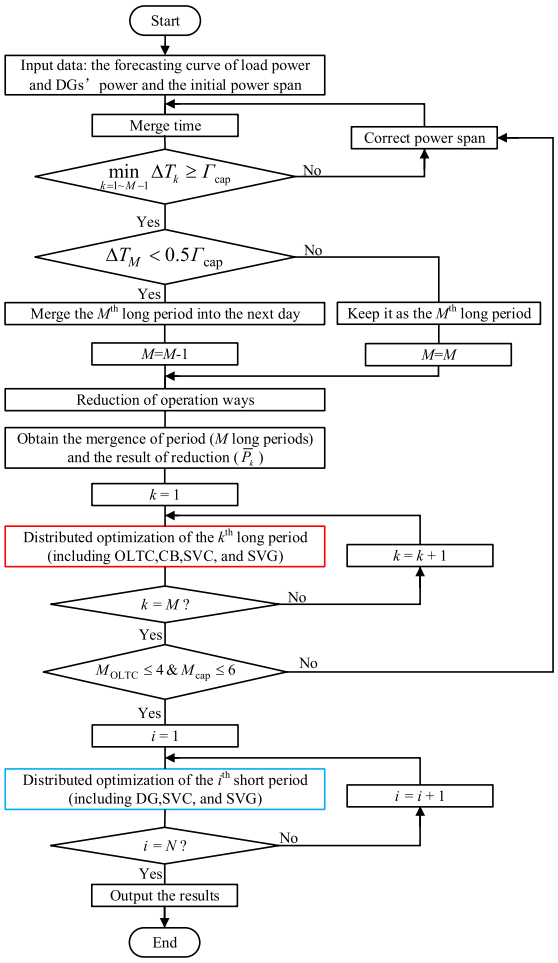

FIGURE 5. Decision-making process of multi-period problem.

The process in Fig. 5 is divided into three main parts:

1) The first part composed of the steps before the red textbox describes the mergence of period and the reduction of operation ways. This part provides calculation data for distributed optimization.

Assume that we extend from the initial load (in Fig. 4) to the right along the net load (which equals load minus DG) curve. It may occur that only the last long period ΔT_k dissatisfies the constraint in (21). (21) can be relaxed to:

$$\min_{k=1\sim M-1} \Delta T_k \geq \Gamma_{\text{cap}} \tag{22}$$

For the last long period ΔT_M, if $\Delta T_M < 0.5\Gamma_{\text{cap}}$, the M^{th} long time period ΔT_M can be merged into the net load cure of the next day, and the number of long time periods is M-1; if $\Delta T_M \geq 0.5\Gamma_{\text{cap}}$, it can be reserved as the M^{th} long time.

2) The second part is the ''rough optimization'' carried out by the red textbox. It mainly focuses on the M long periods and the reduction of operation ways. For every long period, all feasible solutions of Var equipment are obtained by the decision-making method for single time period in Section IV-A.

If the action times of OLTC and capacitor banks solved are within the allowable limits (which are $M_{\text{OLTC}} \leq 4$ and $M_{\text{cap}} \leq 6$ in Fig. 5), the following steps in the blue textbox can be execute; If $M_{\text{OLTC}} > 4$ (or $M_{\text{cap}} > 6$), then re-select P_{span} and merge periods again.

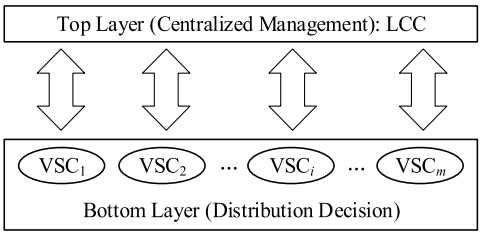

FIGURE 6. Two-layer hybrid control system architecture.

3) The third part is the ''fine optimization'' in the blue textbox. It mainly focuses on the N short periods, and the decision-making method for single period in Section IV-A is adopted. In the third part, the feasible solutions of OLTC and capacitors obtained in 2) remain unchanged, i.e., the ''fine optimization'' is only for DG, SVG and SVC.

In the ''fine optimization'', the priority of SVG/SVC participating in optimization should be higher than DGs' priority in order to avoid affecting the active output of DG. If voltage before the ''fine optimization'' at a node exceeds specified limit with the feasible solutions of OLTC and capacitors obtained in 2), the instruction of target voltage should be executed by following the sequence of SVG/SVC, capacitor, OLTC, and inverter of DG. After the node voltage is corrected, the instruction of the ''fine optimization'' can be executed.

The above process is mainly based on the following ideas:

The ''rough optimization'' for the reduction of operation ways can reduce the computational complexity and efficiently obtain the feasible solutions of OLTC and capacitors which basically reduce loss. However, the optimization results of this process are not fine enough. The ''fine optimization'' in the third part can make up deficiencies of ''rough optimization'' by DG, SVG and SVC due to its fast response.

In summary, the final decision-making results of OLTC and capacitor banks are provided only by the ''rough optimization'' for the long periods. The final results of DG, SVG and SVC are obtained by the ''fine optimization'' for the short periods. The final results of active power loss are also determined by the third part.

V. TWO-LAYER COLLABORATIVE ARCHITECTURE

With the process of DG and distributed technology, the VOC will improve from the centralized mode to the distributed mode or the hybrid model of them. Based on the above ideas, a hybrid mode is constructed shown in Fig. 6.

For DN operating in open loop, LCC is appointed as the top management system in dispatching center or feeder dispatching center of DN. In addition to acquiring data of feeder terminal unit (FTU), transformer terminal unit (TTU), line terminal unit (LTU), and Var terminal unit (VTU), LCC

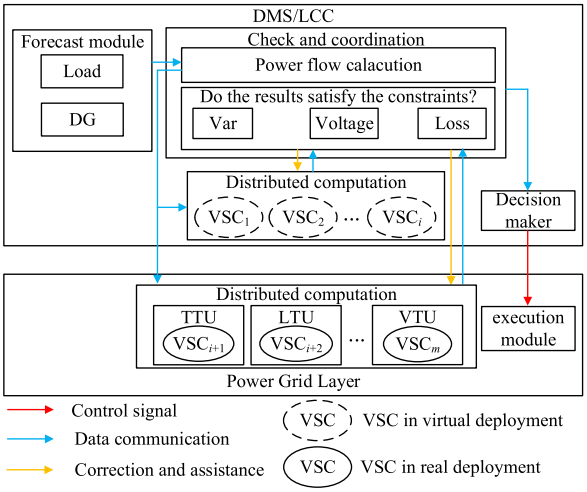

FIGURE 7. The architecture of distributed computation for the D-VOC.

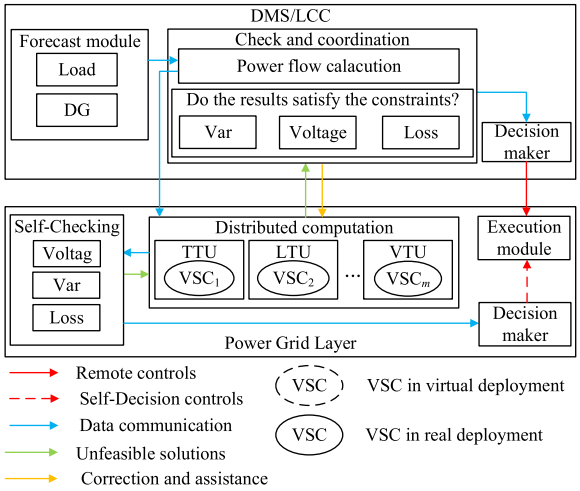

FIGURE 8. The architecture of distributed execution for the VOC.

acquires and picks out information from VSC including its status, autonomous control, and assistance request. Based on various data or information, LCC first verifies the distributed decision-making results of all VSCs and revises the unqualified ones. Then LCC authorizes the VSCs whose results are verified or revised to execute their own operational instructions. The hybrid system architecture no longer requires centralized optimization computation with complex nonlinear mixed integer optimization method or software for large-scale DN.

VSC can be selectively deployed, which depends on the specific demands:

A. DISTRIBUTED COMPUTATION FOR THE D-VOC

This demand only involves the distributed optimization computation; however, the process of instruction execution is still performed according to the existing centralized management mode.

For this demand, VSC can be deployed in virtual or real mode at the node with Var equipment allocating in Fig. 7.

If all hardware and software resources for distributed computation are concentrated in LCC, VSCs are in virtual deployment and a certain amount of computing resources are allocated to VSCs. For virtual deployment, VSC is formally located in the bottom layer of the architecture in Fig. 6. However, the computing entities are actually in the LCC's computing center.

If TTU, LTU, and VTU have distributed computing resources (primarily extended with the distributed computing resources and algorithm), VSCs can be in real deployment based on these units. In this case, all VSCs and their entities are actually in the bottom layer.

B. DISTRIBUTED EXECUTION FOR THE VOC

Unlike A which is restricted to distributed computation, VSC is selectively responsible for distributed execution, in addition to the distributed computation (shown in Fig. 8).

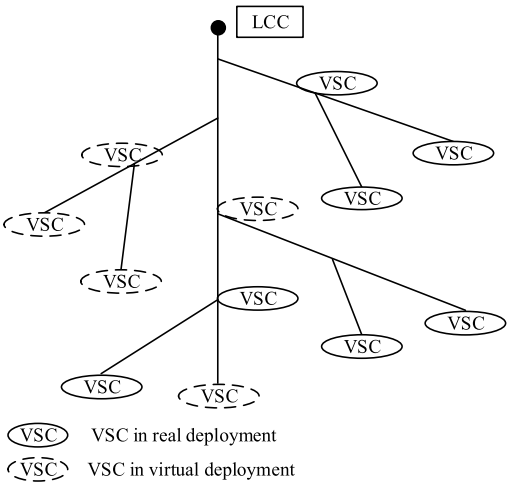

FIGURE 9. Sketch of VSC's arrangement.

Some VSCs are entitled to self-decision and self-execution; Other VSCs are entitled to self-execution. However, the self-decision results must be verified in LCC. The verified decision can be executed by LCC through the remote control or be self-executed by the corresponding VSC through local control. At this time, VSCs are all installed in a real deployment.

In the process of self-decision, VSCs' self-checking mainly includes three aspects according to the control objectives (which described in detail in Section IV-A): VSCs check whether the output of var equipment exceeds the limit, whether the voltage exceeds the limit, and whether the active power loss is minimum for distributed equivalent load system.

In the process of verification, LCC only uses ordinary power flow program to screen out the nodes where the voltages exceed the limits, and requires the corresponding VSCs to revise their decisions (that means re-decision process). If the re-decision is beyond the local control ability, the corresponding VSC will request assistance from nearby VSCs through LCC.

TABLE 1. Installation Information of WDGs.

WDGs Connection Bus	Rate Power (kW)
27	300
54	600
69	700

The mapping relation between VSCs in virtual or real deployment and the network is shown in Fig. 9. Typically, VSC is deployed at node (or the equivalent load node) with Var equipment as needed.

VI. CASE STUDY

A. MODIFIED PG & E 69-BUS DISTRIBUTION SYSTEM

The case study is based on the PG & E 69-bus distribution system (shown in Fig. 15). OLTC between the nodes 0 and 1 is a YNyn0 link three-phase double winding transformer rated at $12.6 \pm 4 \times 2.5\%$ kV. The primary terminal is fixed to 66 kV. Three wind power DGs (WDGs) are connected to DN. The connection buses and rated power are highlighted in Table 1.

Refer to [31], the tables in Appendix A describe the installation information of capacitor banks and SVG. The base values of the system have been assumed as 12.66 kV and 10 MVA. The line power limit is omitted.

The initial states of Var equipment are set: the tap of OLTC is $\pm\ 0 \times 2.5\%$, the switching number of capacitor banks is 0, and the output of SVG is 0 MVar. The daily maximum action times of OLTC and shunt capacitor banks are 4 and 6 times respectively. In addition, let $\Gamma_{\text{oltc}} = 2\text{h}$ and $\Gamma_{\text{cap}} = 1\text{h}$. Daily load power and daily DGs' power forecasting curves are shown in Appendix B.

The optimization targets are to keep voltage within $\pm 7\%$ of 1 p.u. and to minimize active power loss of every equivalent load system by distributed optimization.

B. SIMULATION RESULT

According to the multi-period decision-making scheme of multi-period problem shown in Section IV-B, the short periods are merged and the operation ways decrease. Let $P_{\text{span}} = 0.1526$ p.u. and the initial starting point be 0:00. 24h are merged into 6 unequal long periods, and their corresponding $\bar{P}_k$ are calculated. For all long periods, the "rough optimization" is executed by the decision-making method in Section IV-A for single period. The calculated result of tap is $+2 \times 2.5\%$ in the whole day shown in Fig. 10.

The time division and results of capacitor switching are shown in Fig. 11. It indicates that the switching times of capacitor banks (at nodes 47, 18, 11, or 68) are within the limits.

Keep the optimized results of capacitor and OLTC unchanged. The "fine optimization" is executed for all short periods. The results of SVG's reactive power (shown in Fig. 12) are calculated to control voltage and reduce active power loss more precisely. The process of iteration for computing B_2 or K is shown in detail in Appendix E.

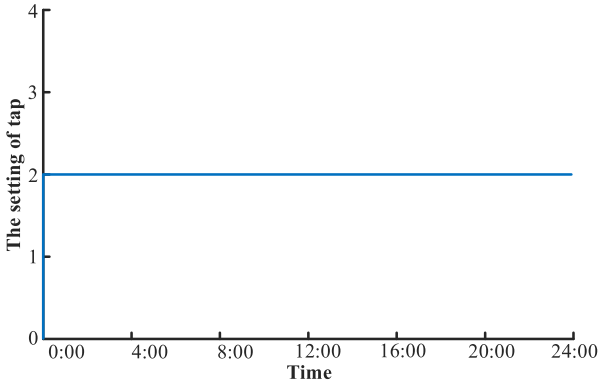

FIGURE 10. Tap changer operations of OLTC.

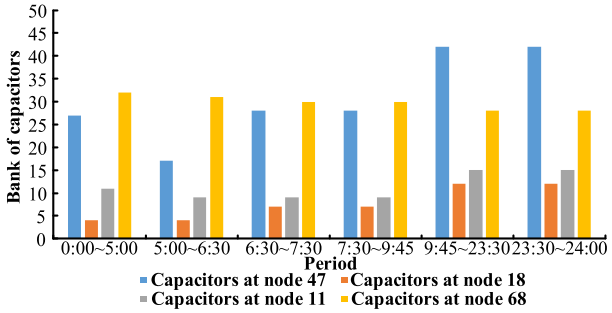

FIGURE 11. Time division and capacitor switching.

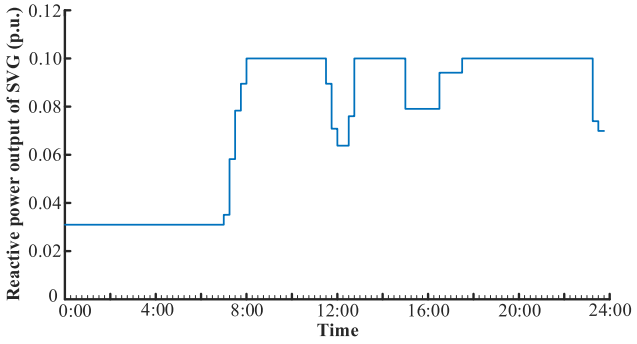

FIGURE 12. Reactive power output of SVG.

The load curve in Fig. 16 shows that the peak mainly occurs in 3 periods, including 10:00-11:30, 13:30-14:00, and 18:30-21:00. Fig. 11 and Fig. 12 illustrate that the outputs of capacitor banks and SVG increase in the peak hours and decrease in the off-peak hours. It can preliminarily demonstrate that the distributed decision-making method in this paper can reasonably dispatch Var equipment in the system. The next part will provide a detailed analysis of the optimization results.

C. RESULT ANALYSIS

From the perspective of active power loss, it indicates that the Var equipment is reasonably scheduled, and the loss is significantly reduced. In Fig. 13, the variation of loss is emphasized.

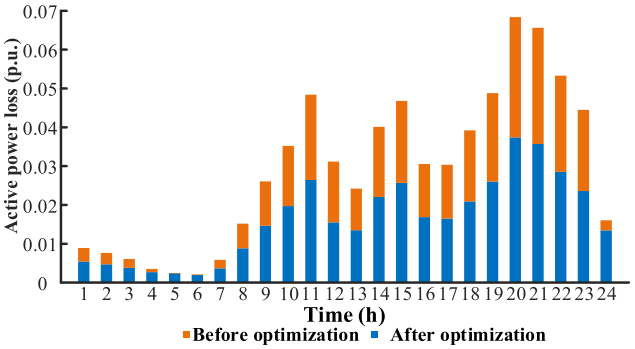

FIGURE 13. Change of active power loss before and after optimization.

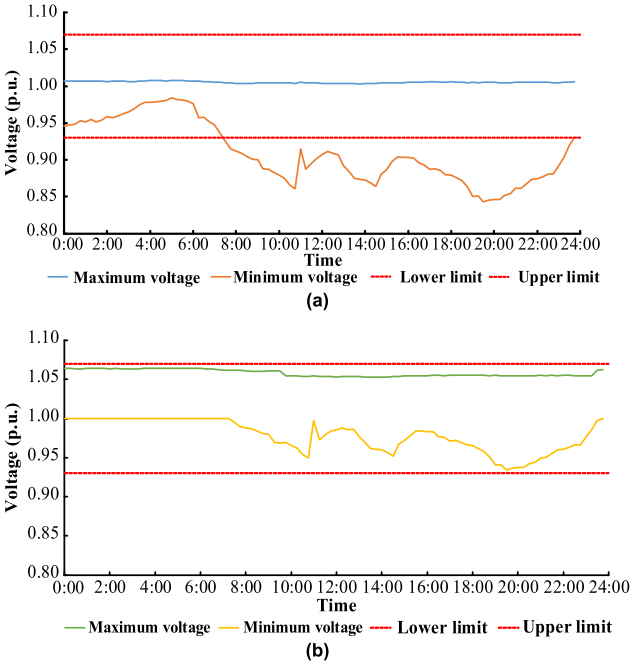

FIGURE 14. Variation of voltage: (a) Before distributed optimization. (b) After distributed optimization.

The loss before optimization in Fig. 13 is gained in the initial state given in Section IV-A. It shows that the loss decreases more obviously in the peak hours.

From the variation of voltage, the profile of maximum and minimum voltage before optimization is shown in Fig. 14(a). From 7:00 to 24:00, the voltage is out-of-limit severely, which will harm the operation of system.

Fig. 14(b) shows the profile of maximum and minimum voltage after optimization. The original problem of voltage is completely eliminated. In addition, the outputs of the Var equipment do not reach the maximum capacity. Moreover, there is a certain margin between voltage profile and the upper/lower limit, which ensures the safety of the system operation.

In addition to the excellent effects of active power loss and voltage control, the method has the advantage of computing performance. Compared with traditional mathematical programming and artificial intelligence algorithms which rely on large-scale mathematical models and complex calculations, the distributed decision-making method in this paper is only for the very simple VSC, a subsystem, in which variables to be optimized are only B_2 and K, and the basic formulas for this work only include (9), (11) and (16). Moreover, the check in LCC is only based on power flow program. Therefore, the new method requires very low computational resources, which are the basis to ensure higher computing performance. The main reasons are:

The optimization process of all existing algorithms is to find a right search direction and determine an appropriate control increment along that direction in each iteration. First, in the process of distributed optimization, each VSC can quickly obtain the right search direction from the perspective of physics (based on local information) rather than mathematical gradient or probability. Second, the step-size of control increment determined by distributed optimization is more efficient than the one determined by mathematical programming or artificial intelligence algorithms. The distributed optimization of VSC can eliminate the unfavorable interference of various non-primary factors in the mathematical gradient or the uncertainty of the probability information in the process of intelligent search. Consequently, VSCs can realize optimization efficiently according to the main or the most important factors relevant to physics. These features make the distributed optimization in this paper more advantageous in computing performance.

VII. CONCLUSION

This paper proposed a distributed decision-making method for VOC in a two-layer collaborative architecture. The case study for the modified PG & E 69-bus distribution grid is accomplished. The conclusion can be drawn:

1) The local decision-makings of VSCs play an important role in making the optimization algorithm effective in the bottom layer. Under the supervision of LCC, the coordination of VSCs can develop full ability of Var equipment.

2) The multi-period decision-making scheme can accomplish the rough and fine optimizations in two stages respectively for the long and short periods. The scheme can not only simplify calculation but also obtain the results of loss reduction and voltage control. Moreover, the action times of OLTC and capacitor banks are within the allowable range, which improves the service life of them.

3) The proposed method based on two-layer collaborative architecture occupies fewer computing resources and has a satisfactory performance of fast computation speed.

This paper has demonstrated that the two-layer collaborative architecture is suitable to D-VOC in DN. The follow-up study will extend this architecture to transmission networks.

APPENDIX

A. INSTALLATION INFORMATION

See Tables 2 and 3.

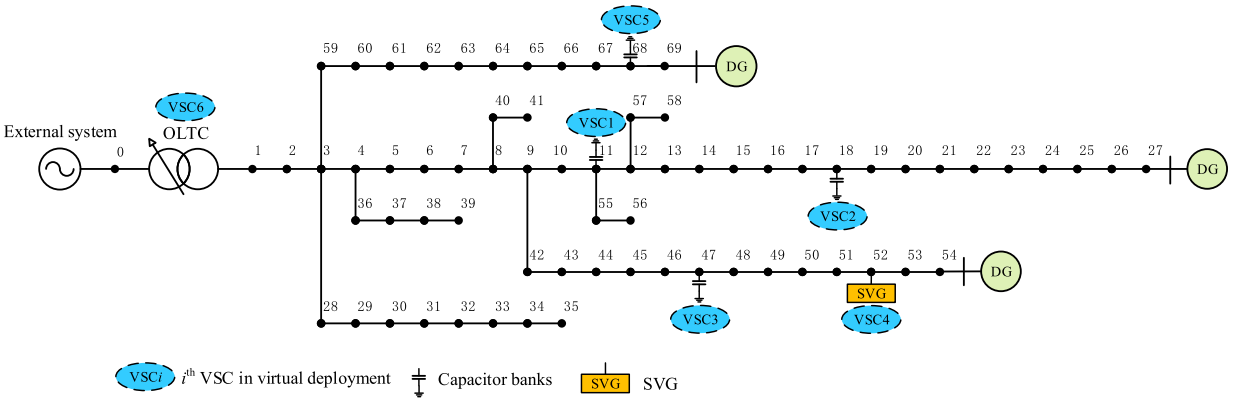

FIGURE 15. Modified PG & E 69-bus distribution grid.

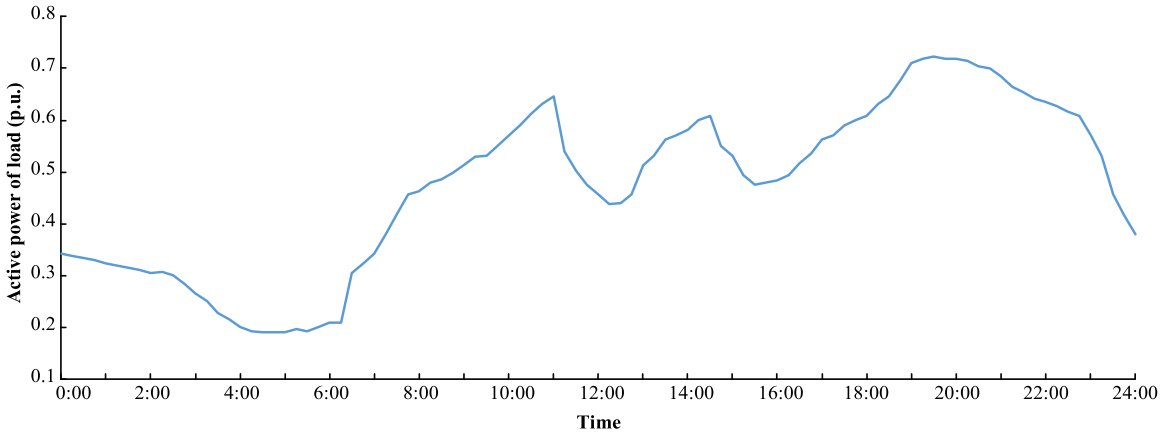

FIGURE 16. Daily load power forecasting curve.

TABLE 2. Installation information of capacitor banks.

Connection Bus	Rated Power (kVar)	Number
18, 11, 47, 68	20	50

TABLE 3. Installation information of SVG.

Connection Bus	Compensation Range (MVar)
52	[-1, 1]

B. DISTRIBUTION SYSTEM FOR CASE STUDY AND FORECASTING CURVES

See Figures 15–17.

C. DERIVATION PROCESS OF (12)

In the equivalent load system with OLTC (in Fig. 1), the equivalent impedance and admittance of the equivalent load are Z_2 and Y_2 respectively, which both satisfy:

$$\begin{cases} R_2 = \dfrac{G_2}{G_2^2 + B_2^2} \\ X_2 = \dfrac{-B_2}{G_2^2 + B_2^2} \end{cases} \tag{C1}$$

According to the definition of Section III, $R = R_1 + KR_2$, and $X = X_1 + KX_2$, so the following formulas can be obtained by using (C1)

$$\begin{cases} \dfrac{R}{X} = \dfrac{R_1 + K\frac{G_2}{G_2^2+B_2^2}}{X_1 + K\frac{-B_2}{G_2^2+B_2^2}} = \dfrac{R_1(G_2^2+B_2^2)+KG_2}{X_1(G_2^2+B_2^2)-KB_2} \\ \dfrac{X}{R} = \dfrac{X_1 + K\frac{-B_2}{G_2^2+B_2^2}}{R_1 + K\frac{G_2}{G_2^2+B_2^2}} = \dfrac{X_1(G_2^2+B_2^2)-KB_2}{R_1(G_2^2+B_2^2)+KG_2} \end{cases} \tag{C2}$$

Substituting (C2) into (11) can obtain the following formulas

$$B_2 = \begin{cases} \dfrac{R_1(G_2^2+B_2^2)+KG_2}{X_1(G_2^2+B_2^2)-KB_2} G_2 \\ -\dfrac{X_1(G_2^2+B_2^2)-KB_2}{R_1(G_2^2+B_2^2)+KG_2} G_2 \end{cases} \tag{C3}$$

Then (12) can be obtained by introducing the iteration number q.

D. PRINCIPLE OF OPTIMALITY

The distributed optimization proposed in this paper is a kind of dynamic programming (DP) technique. It complies with Principle of Optimality.

DP technique rests on principle of optimality. Roughly, it states the following rather obvious fact [32].

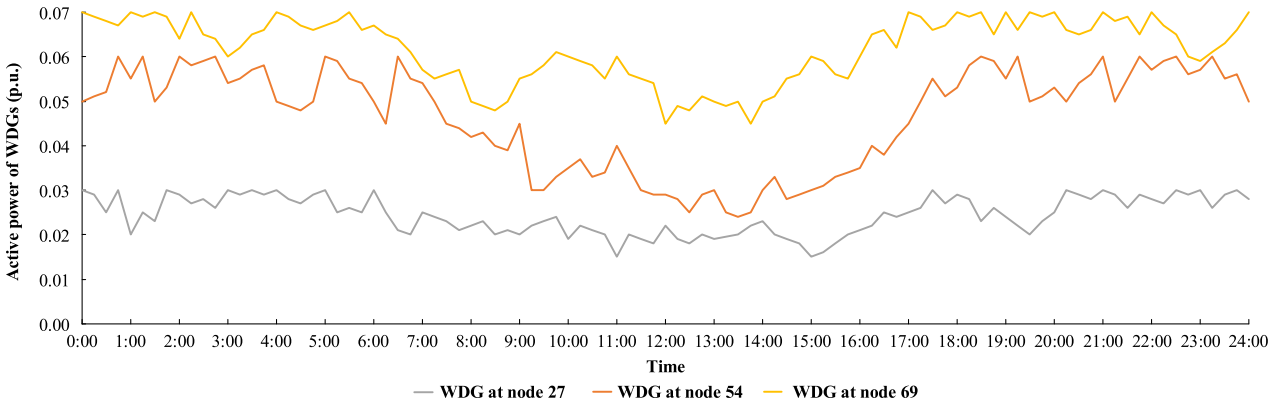

FIGURE 17. Daily DGs' power forecasting curve.

Theorem 1 Principle of Optimality

Let $\pi^* = \{\mu_0^*, \mu_1^*, \ldots, \mu_{N-1}^*\}$ be an optimal strategy for the basic problem, and assume that when using π^*, a given state x_i occurs at time i with positive probability. Consider the subproblem whereby we are at x_i at time i and wish to minimize the "cost-to-go" from time i to time N

$$E\left\{g_N(x_N) + \sum_{k=i}^{N-1} g_k(x_k, \mu_k(x_k), \omega_k)\right\} \quad \text{(D1)}$$

Then the truncated strategy $\{\mu_i^*, \mu_{i+1}^*, \ldots, \mu_{N-1}^*\}$ is optimal for this subproblem.

The principle of optimality suggests that an optimal strategy can be constructed in piecemeal fashion, first constructing an optimal strategy for the "tail subproblem" involving the last two stages, and continuing in this manner until an optimal strategy for the entire problem is constructed. DP algorithm is based on this idea: it proceeds sequentially, by solving all the tail subproblems of a given time length.

It is noticeable that the problem can be solved by starting with the subprocess (or the subsystem). Under the condition that the state variables of the input are different, we start from the last subsystem, and analyze the value of control variables for optimizing subprocess (or subsystem). Then, according to the input variables of the whole system and the analysis result of the subsystem, the optimal decision of control variables in each process or each system is finally determined.

Extend from subsystem (or subprocess) to entire system (or the whole process). A large-scale system (or a big problem) can be decomposed into several subsystems (or subproblems), which can simplify calculation.

VSCs are the subsystems of the whole system to be optimized in this paper. We can easily obtain the optimal control variables B_2 and K of VSCs, subsystems, by using Kuhn-Tucker condition. Then, according to the input parameters (including the results of power flow) of DN and the optimized results of all VSCs, the optimal decision of control variables in each process for the whole system is finally determined. After iterations for minimum power loss in each VSC, subsystem, loss of the whole distribution system can quickly decrease and converge to the final optimal solution.

TABLE 4. Initial values of variables.

Variables	Initial Values
Voltage Corresponding to Each VSC (p.u.)	$U_{2(11)} = 0.9862$, $U_{2(18)} = 0.9845$, $U_{2(47)} = 0.9669$, $U_{2(52)} = 0.9599$, $U_{2(68)} = 1.0046$
Active Power Loss (p.u.)	$P_{\text{loss}} = 0.0066$

TABLE 5. Values of variables after the adjustment of OLTC.

Variables	Values
Voltage Corresponding to Each VSC (p.u.)	$U_{2(11)} = 1.0369$, $U_{2(18)} = 1.0353$, $U_{2(47)} = 1.0186$, $U_{2(52)} = 1.0120$, $U_{2(68)} = 1.0544$
Active Power Loss (p.u.)	$P_{\text{loss}} = 0.0060$

E. PROCESS OF ITERATION

In Section VI, "rough optimization" aims to keep voltage in [0.93, 1.07] p.u. and minimize the active power loss for every equivalent load system. Take one period as an example. The influence of variables on the optimization results will be described in detail below.

For 0:00-5:00, the initial values of voltage corresponding to each VSC and active power loss are shown in Table 4 where $U_{2(i)}$ is the voltage of node i and P_{loss} is the active power loss.

By formula (9), calculate and select the value closest to 1.0 as the result of K. After the adjustment of OLTC, the voltage corresponding to each VSC and active power loss are shown in Table 5.

Based on the state in Table 5, further distributed optimization is accomplished by controlling other VSCs in the grid. The VSCs corresponding to capacitor banks and SVG accomplish distributed optimization at the same time. In each VSC, subsystem (mentioned in Appendix D), LCC checks results by power flow calculation, observes the variation of voltage and active power loss, and selects the optimal solution which satisfies the optimization objectives.

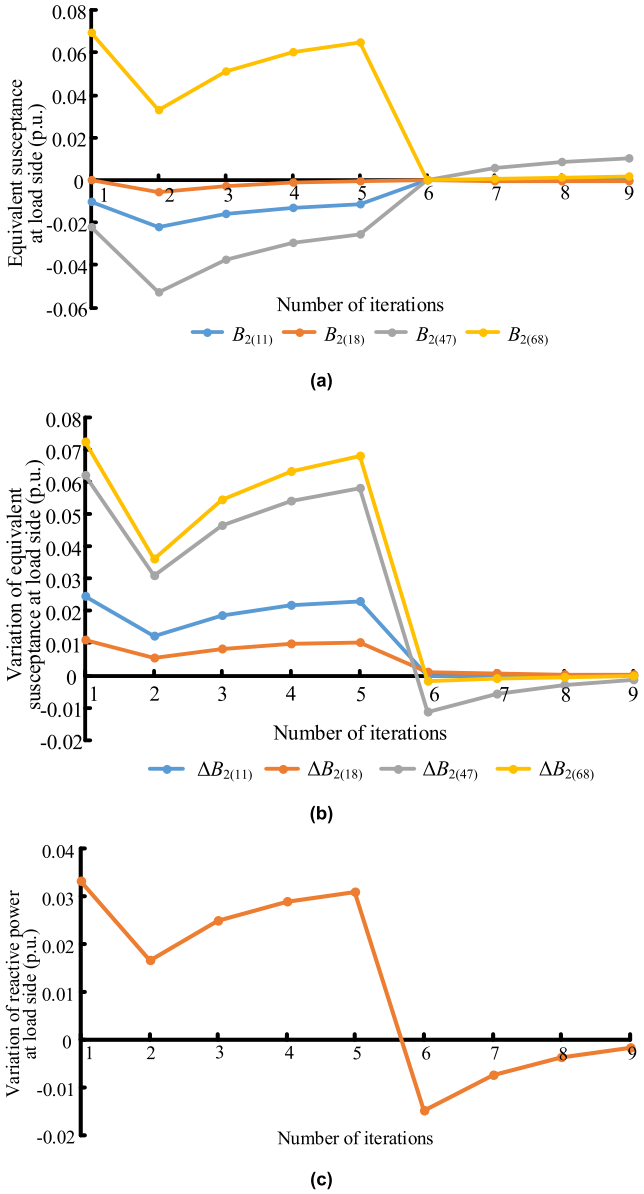

FIGURE 18. Variation of variables in iterative process: (a) Equivalent susceptance B_2 at load side. (b) Variation of equivalent susceptance ΔB_2. (c) Variation of reactive power ΔQ_2 at load side.

In the process of optimization, the values of variables are shown in Fig. 18. In Fig. 18(a), (b) and (c), the values corresponding to each initial number constitute the first set of VSCs' results, and so on. In Fig. 18(a) and (b), $B_{2(i)}$ is equivalent susceptance at load side of node i; $\Delta B_{2(i)}$ is the variation of $B_{2(i)}$. The switching of the capacitor bank at node i can be calculated by $\Delta B_{2(i)}$. Fig. 18(c) shows the values of the variables of node 52 during iterative process. In Fig. 18(c), ΔQ_2 is the variation of $Q_{2(i)}$, and $Q_{2(i)}$ is the reactive power of the equivalent system at load side of node i. The output of SVG at node 52 can be calculated by ΔQ_2.

In iterative process, the active power loss, maximum voltage, and minimum voltage are shown in Table 6. According to the results in Fig. 18, the target variables are obtained by power flow calculation. In Table 6, the 2nd row is corresponding to the first set of VSCs results and so on. The initial system state corresponding to the 2nd row of Table 6 is that OLTC tap is set at $\pm 2 \times 2.5\%$, the switching number of capacitor banks is 0, and the output of SVG is 0 MVar. The initial system state corresponding to the 7th row of Table 6 is the system state after optimization corresponding to the first set of results. After one iteration, the value of P_{loss} may not be a local optimal solution. The increment of variables (including ΔB_2 and ΔQ_2) may appropriately decrease or increase to calculate the new value of P_{loss} (shown from the 3rd to 6th row, and from the 8th to 9th row in Table 6). LCC selects the smallest P_{loss}, and finally determines the local optimal solution.

TABLE 6. Values of target variables.

Number	Active power loss (p.u.)	Minimum voltage (p.u.)	Maximum voltage (p.u.)
1	0.0033	1.0000	1.0627
2	0.0037	1.0000	1.0585
3	0.0033	1.0000	1.0606
4	0.0032	1.0000	1.0618
5	0.0033	1.0000	1.0622
6	0.0035	1.0000	1.0622
7	0.0034	1.0000	1.0627
8	0.0033	1.0000	1.0627
9	0.0033	1.0000	1.0627

For the rest of the periods, the "rough optimization" can be accomplished according to the process mentioned above. The "fine optimization" can be accomplished according to the optimization of SVG.

REFERENCES

[1] G. Cavraro and R. Carli, "Local and distributed voltage control algorithms in distribution networks," *IEEE Trans. Power Syst.*, vol. 33, no. 2, pp. 1420–1430, Mar. 2018.
[2] A. Keane, L. F. Ochoa, C. L. T. Borges, G. W. Ault, A. D. Alarcon-Rodriguez, R. A. F. Currie, F. Pilo, C. Dent, and G. P. Harrison, "State-of-the-art techniques and challenges ahead for distributed generation planning and optimization," *IEEE Trans. Power Syst.*, vol. 28, no. 2, pp. 1493–1502, May 2013.
[3] M. Bahramipanah, D. Torregrossa, R. Cherkaoui, and M. Paolone, "A decentralized adaptive model-based real-time control for active distribution networks using battery energy storage systems," *IEEE Trans. Smart Grid*, vol. 9, no. 4, pp. 3406–3418, Jul. 2018.
[4] Y. Liu, Z. Qu, H. Xin, and D. Gan, "Distributed real-time optimal power flow control in smart grid," *IEEE Trans. Power Syst.*, vol. 32, no. 5, pp. 3403–3414, Sep. 2017.
[5] S. O. Muhanji, A. Muzhikyan, and A. M. Farid, "Distributed control for distributed energy resources: Long-term challenges and lessons learned," *IEEE Access*, vol. 6, pp. 32737–32753, 2018.
[6] M. Chamana, B. H. Chowdhury, and F. Jahanbakhsh, "Distributed control of voltage regulating devices in the presence of high PV penetration to mitigate ramp-rate issues," *IEEE Trans. Smart Grid*, vol. 9, no. 2, pp. 1086–1095, Mar. 2018.
[7] B. P. Hayes and M. Prodanovic, "State forecasting and operational planning for distribution network energy management systems," *IEEE Trans. Smart Grid*, vol. 7, no. 2, pp. 1002–1011, Mar. 2016.
[8] T. Sansawatt, L. F. Ochoa, and G. P. Harrison, "Smart decentralized control of DG for voltage and thermal constraint management," *IEEE Trans. Power Syst.*, vol. 27, no. 3, pp. 1637–1645, Aug. 2012.
[9] K. E. Antoniadou-Plytaria, I. N. Kouveliotis-Lysikatos, P. S. Georgilakis, and N. D. Hatziargyriou, "Distributed and decentralized voltage control of smart distribution networks: Models, methods, and future research," *IEEE Trans. Smart Grid*, vol. 8, no. 6, pp. 2999–3008, Nov. 2017.

[10] H. Xia, Q. Li, R. Xu, T. Chen, J. Wang, M. A. S. Hassan, and M. Chen, "Distributed control method for economic dispatch in islanded microgrids with renewable energy sources," *IEEE Access*, vol. 6, pp. 21802–21811, 2018.

[11] A. Borghetti, "Using mixed integer programming for the volt/var optimization in distribution feeders," *Electr. Power Syst. Res.*, vol. 98, pp. 39–50, May 2013.

[12] S. R. Shukla, S. Paudyal, and M. R. Almassalkhi, "Efficient distribution system optimal power flow with discrete control of load tap changers," *IEEE Trans. Power Syst.*, vol. 34, no. 4, pp. 2970–2979, Jul. 2019.

[13] M. B. Liu, C. A. Canizares, and W. Huang, "Reactive power and voltage control in distribution systems with limited switching operations," *IEEE Trans. Power Syst.*, vol. 24, no. 2, pp. 889–899, May 2009.

[14] A. Abessi, V. Vahidinasab, and M. S. Ghazizadeh, "Centralized support distributed voltage control by using end-users as reactive power support," *IEEE Trans. Smart Grid*, vol. 7, no. 1, pp. 178–188, Jan. 2016.

[15] V. Parada, J. A. Ferland, M. Arias, and K. Daniels, "Optimization of electrical distribution feeders using simulated annealing," *IEEE Trans. Power Del.*, vol. 19, no. 3, pp. 1135–1141, Jul. 2004.

[16] H. Pezeshki, A. Arefi, G. Ledwich, and P. Wolfs, "Probabilistic voltage management using OLTC and dSTATCOM in distribution networks," *IEEE Trans. Power Del.*, vol. 33, no. 2, pp. 570–580, Apr. 2018.

[17] A. P. S. Meliopoulos, E. Polymeneas, Z. Tan, R. Huang, and D. Zhao, "Advanced distribution management system," *IEEE Trans. Smart Grid*, vol. 4, no. 4, pp. 2109–2117, Dec. 2013.

[18] H. Gao, J. Liu, L. Wang, and Z. Wei, "Decentralized energy management for networked microgrids in future distribution systems," *IEEE Trans. Power Syst.*, vol. 33, no. 4, pp. 3599–3610, Jul. 2018.

[19] D. K. Molzahn, F. Dörfler, H. Sandberg, S. H. Low, S. Chakrabarti, R. Baldick, and J. Lavaei, "A survey of distributed optimization and control algorithms for electric power systems," *IEEE Trans. Smart Grid*, vol. 8, no. 6, pp. 2941–2962, Nov. 2017.

[20] W. U. Hongbin, C. Huang, M. Ding, B. Zhao, and P. Li, "Distributed cooperative voltage control based on curve-fitting in active distribution networks," *J. Modern Power Syst. Clean Energy*, vol. 5, no. 5, pp. 777–786, Oct. 2017.

[21] Y. Xu and H. Sun, "Distributed finite-time convergence control of an islanded low-voltage AC microgrid," *IEEE Trans. Power Syst.*, vol. 33, no. 3, pp. 2339–2348, May 2018.

[22] V. Calderaro, G. Conio, V. Galdi, G. Massa, and A. Piccolo, "Optimal decentralized voltage control for distribution systems with inverter-based distributed generators," *IEEE Trans. Power Syst.*, vol. 29, no. 1, pp. 230–241, Jan. 2014.

[23] B. A. Robbins, C. N. Hadjicostis, and A. D. Domínguez-García, "A two-stage distributed architecture for voltage control in power distribution systems," *IEEE Trans. Power Syst.*, vol. 28, no. 2, pp. 1470–1482, May 2013.

[24] P. Pachanapan, O. Anaya-Lara, A. Dysko, and K. L. Lo, "Adaptive zone identification for voltage level control in distribution networks with DG," *IEEE Trans. Smart Grid*, vol. 3, no. 4, pp. 1594–1602, Dec. 2012.

[25] H. S. Bidgoli and T. Van Cutsem, "Combined local and centralized voltage control in active distribution networks," *IEEE Trans. Power Syst.*, vol. 33, no. 2, pp. 1374–1384, Mar. 2018.

[26] A. G. Beccuti, T. H. Demiray, G. Andersson, and M. Morari, "A Lagrangian decomposition algorithm for optimal emergency voltage control," *IEEE Trans. Power Syst.*, vol. 25, no. 4, pp. 1769–1779, Nov. 2010.

[27] X. Zhang, A. J. Flueck, and C. P. Nguyen, "Agent-based distributed volt/var control with distributed power flow solver in smart grid," *IEEE Trans. Smart Grid*, vol. 7, no. 2, pp. 600–607, Mar. 2016.

[28] A. Borghetti, R. Bottura, M. Barbiroli, and C. A. Nucci, "Synchrophasors-based distributed secondary voltage/VAR control via cellular network," *IEEE Trans. Smart Grid*, vol. 8, no. 1, pp. 262–274, Jan. 2017.

[29] M. Bahramipanah, R. Cherkaoui, and M. Paolone, "Decentralized voltage control of clustered active distribution network by means of energy storage systems," *Electr. Power Syst. Res.*, vol. 136, pp. 370–382, Jul. 2016.

[30] H. Sun, Q. Guo, J. Qi, V. Ajjarapu, R. Bravo, J. Chow, Z. Li, R. Moghe, E. Nasr-Azadani, U. Tamrakar, G. N. Taranto, R. Tonkoski, G. Valverde, Q. Wu, and G. Yang, "Review of challenges and research opportunities for voltage control in smart grids," *IEEE Trans. Power Syst.*, vol. 34, no. 4, pp. 2790–2801, Jul. 2019.

[31] M. E. Baran and F. F. Wu, "Optimal capacitor placement on radial distribution systems," *IEEE Trans. Power Del.*, vol. 4, no. 1, pp. 725–734, Jan. 1989.

[32] R. Bellman, *Dynamic Programming* (Dover Books on Computer Science). New York, NY, USA: Dover, 2013.

QIYI YU received the B.S. degree in electrical engineering from Shandong University, Jinan, China, in 2017. She is currently pursuing the M.S. degree with the School of NARI Electric and Automation, Nanjing Normal University, China. Her main research interest includes distributed volt/var control.

QI WANG received the B.S., M.S., and Ph.D. degrees in electrical engineering from the Harbin Institute of Technology, Harbin, China, in 1998, 2003, and 2008, respectively. From September 2010 to January 2013, she held a postdoctoral position with Hohai University, Nanjing, China, and from 2013 March to September 2013, she was a Visiting Scholar with Northumbria University, Newcastle, U.K. Since 1998, she has been with the School of Electrical and Automation Engineering, Nanjing Normal University, Nanjing, where she is currently an Associate Professor. Her current research interests include optimization of power systems, renewable energy generation, and application of power electronics in the power systems.

WEI LI received the Ph.D. degree. He is currently a Senior Engineer with NARI Group Corporation, Nanjing, China. His research interests include stability analysis and control of power grid.

FUSUO LIU received the Ph.D. degree. He is currently a Senior Engineer with NARI Group Corporation, Nanjing, China, where he is also a Manager with the Department of Electric Network Analysis. His research interests include stability analysis and control of power grid.

ZHONGYU SHEN received the B.S. degree in automation engineering from Nanjing Tech University, Nanjing, China, in 1983, and the M.S. degree in automation engineering from the East China University of Science and Technology, Shanghai, China, in 1991. Since 2000, he has been with the School of Electrical and Automation Engineering, Nanjing Normal University, Nanjing, where he is currently a Professor. His current research interests include detection technology, application of automation equipment, and control system simulation technology.

JIAQI JU received the B.S. degree in electrical engineering from Nanjing Normal University, Nanjing, China, in 2016, where she is currently pursuing the Ph.D. degree with the School of Electric and Automation. Her main research interests include integrated energy systems, information network security, and cyber-physical systems.